

U.S. PATENT OFFICE
UN-P-93/24
MAY 1974

**Comparison of Lead Zirconate Titanate Thin Films on
Ruthenium Oxide and Platinum Electrodes**

L.A. Bursill* and Ian M. Reaney

*Laboratoire de Ceramique, MX-D, Ecole Polytechnique
Federale de Lausanne, Ecublens, CH-1015, Suisse*

and

D.P. Vijay and S.B. Desu

*Department of Materials Science and Engineering
Virginia Polytechnique Institute and State University
Blacksburg, VA 24061, U.S.A.*

Received to be inserted
Revised to be inserted

Abstract

High-resolution and bright- and dark-field transmission electron microscopy are used to characterize and compare the interface structures and microstructure of PZT/RuO₂/SiO₂/Si and PZT/Pt/Ti/SiO₂/Si ferroelectric thin films, with a view to understanding the improved fatigue characteristics of PZT thin films with RuO₂ electrodes. The RuO₂/PZT interface consists of a curved pseudoperiodic minimal surface. The interface is chemically sharp with virtually no intermixing of RuO₂ and PZT, as evidenced by the atomic resolution images as well as energy dispersive X-ray analysis. A nanocrystalline pyrochlore phase Pb₂ZrTiO_{7-x} x≠1 was found on the top surface of the PZT layer. The PZT/Pt/Ti/SiO₂/Si thin film was well-crystallized and showed sharp interfaces throughout. Possible reasons for the improved fatigue characteristics of PZT/RuO₂/SiO₂/Si thin films are discussed in the text.

1. INTRODUCTION

Interface related degradation problems of ferroelectric $\text{PbZr}_{0.53}\text{Ti}_{0.47}$ thin film switching characteristics led to the search for alternate electrode materials to replace the conventional platinum electrodes. The suitability of the ceramic conducting electrodes ruthenium dioxide (RuO_2) and indium-tin-oxide (ITO) was examined by Vijay and Desu¹. Thin films of RuO_2 and ITO were deposited onto Si/SiO_2 substrates by reactive sputtering. Sol-gel derived PZT thin films were deposited onto the conducting electrodes and the samples annealed at various temperatures between 400 and 700C. Less intermixing was observed for the $\text{Si}/\text{SiO}_2/\text{RuO}_2/\text{PZT}$ films than for $\text{Si}/\text{SiO}_2/\text{ITO}/\text{PZT}$ after similar PZT processing. The ferroelectric properties of the PZT films, i.e. hysteresis, fatigue and low voltage breakdown, were also compared for the two sets of electrodes. Improved fatigue properties were observed for the RuO_2 electrodes. The latter also showed better current-voltage (I-V) and time dependent dielectric breakdown properties (TDDB). Earlier studies of RuO_2 electrodes on PZT were reported by Yoo and Desu^{2,3} and Vijay, Pan, Yoo and Desu⁴. RuO_2 is more readily etched than is Pt; which is interesting for potential VLSI integration of PZT thin films.

The purpose of the present work was to compare the PZT/electrode interface structures for RuO_2 and Pt electrodes; with respect to understanding the different degradation properties for Pt and RuO_2 . According to a theoretical model for degradation of oxide ferroelectrics due to Desu and Yoo⁵, the structure of the PZT/electrode is assumed to have the major effect on the degradation properties, i.e. on fatigue, ageing and I-V characteristics, of a ferroelectric capacitor. That model assumed that oxygen vacancy migration and trapping at the PZT/electrode interface is responsible for loss of switchable polarization after repeated switching (fatigue). Experiments showed that RuO_2 electrodes gave much reduced fatigue, compared to Pt (Vijay and Desu¹), which was attributed to increased stability of the RuO_2/PZT interface resulting from reduced lattice mismatch, a more favorable contact potential and a sharp interface structure, with virtually no interdiffusion of PZT/ RuO_2 .

It was proposed that such increased stability reduces any tendency for oxygen vacancy migration and subsequent trapping at the interface. Vijay and Desu¹ suggested that the composition gradient is reduced for PZT/ RuO_2 by formation of a thin layer of a $\text{Pb}_2\text{Ru}_2\text{O}_{7-r}$ pyrochlore phase at the interface due to a limited extent of chemical mixing during the 650C 30min annealing required to crystallize the PZT.

The original aim of the present study was to attempt to detect this compound using high-resolution transmission electron microscopy (HRTEM); it was also interesting to compare, as directly as possible, the interface structures of PZT/Pt and PZT/RuO₂ capacitors. The results of HRTEM, as well as classical bright- and dark-field TEM and some analytical electron microscopy are reported below.

II. EXPERIMENTAL

A. Fabrication details

Bare Si(100) wafers were first oxidised in an atmosphere of wet oxygen at 950C to form the amorphous SiO₂ barrier layers. This is to prevent contact between Pt and Si, which would otherwise form complex platinum silicides⁶. An additional thin Ti layer was sputtered onto the silica to improve adhesion of Pt to the silica substrate⁷. This was not necessary for RuO₂ on silica.

RuO₂ electrodes were sputtered reactively onto the Si/SiO₂ substrate using a ruthenium metal target in an atmosphere of oxygen/argon in the ratio 1:4; the gas pressure was 10mTorr during sputtering with a current of 0.2amps. The Pt electrode was also deposited onto the Si/SiO₂/Ti substrate using a DC magnetron sputterer in an atmosphere of argon.

The PbZr_xTi_{1-x}O₃, x=0.53 precursor solution was prepared by a sol-gel technique from a metallorganic solution of Zr-iso-propoxide, Ti-n-propoxide and Pb-acetate. 10 percent excess Pb was added to the solution to compensate for the expected loss of lead during crystallization of the PZT at 650C. The solution was hydrolyzed to form the precursor with a concentration of 0.4M. PZT thin films were spin-coated onto the electrodes; with adjustment of the number of coatings and speed of coating to obtain the desired thickness of 400nm. The coated films were dried in air.

These as-deposited films were amorphous. PZT was crystallized by annealing at 650C for 30min in a quartz tube furnace, in air. Fig.1 shows chemical details as well as dimensional specifications of the two thin films studied herein.

B. Electron microscopy.

Four pieces each 3mm square were cleaved from the two PZT/electrode specimens. These were glued together using an epoxy resin as a stack with two pairs of PZT surfaces facing inwards. These sandwiches were ground mechanically using fine grade silicon carbide paper in such a way as to produce transverse cross-sections 30 micron deep. A 2.3mm copper specimen support ring was glued to one surface and the sample ion-thinned from both sides at an angle of incidence of 15 degree. This is a modification of a technique developed for ferroelectric thin films by Reaney and Barber⁸; see also Sreenivas, Reaney, Maeder, Setter, Jacadish and Elliman⁹.

The thin specimens were examined using a Philips EM430 300keV HRTEM instrument at Institut Interdepartementale de Microscopie Electronique (I2M), EPFL. Observations were made at close to room temperature using a +/- 10 degree double-tilt goniometer. The instrumental resolution was significantly better than 0.2nm although the interpretable structure resolution was limited to 0.2nm, since the spherical aberration coefficient was 1.2mm. Selected area diffraction patterns were recorded using the smallest projector lens aperture, when the effective beam diameter at the specimen plane was about 100nm.

Some energy dispersive X-ray spectroscopy (EDX) analysis was made using a Hitachi 2000-HF field-emission analytical electron microscope at 200keV, also at I2M.

III. RESULTS

A. PZT/RuO₂/SiO₂/Si

Fig.2 shows an overall view of one thin film cross-section; from left to right may be seen crystalline Si/ amorphous SiO₂/ columnar crystallites of RuO₂/ crystallized PZT/ and amorphous epoxy. This is a dark-field image with objective aperture centered over the polycrystalline electron diffraction ring pattern (Fig.3). The PZT portion consists of grains some 25nm diameter. The RuO₂ layer is well crystallized, indicated by extensive arrays of lattice fringes; shown in the enlargement of Fig.2 given as Fig.4. It has a pronounced columnar texture, where each grain (about 5nm wide) extends throughout the thickness of the RuO₂ layer (about 250nm thick). Extensive arrays of 0.5nm fringes may be seen in the RuO₂ grains, indicating perhaps some preferred orientation. Further enlargement of the RuO₂/PZT interface (Fig.5) shows that this interface is not flat; it consists of a series of roughly periodic curved boundaries reflecting the

shape of the outer surface of the columnar grains of RuO₂. Fig.6 is a HRTEM image showing atomic resolution detail of two such curved segments. The PZT appears well-crystallized; it is oriented with (100) lattice planes parallel to the original substrate in this case. Note that there is no evidence for an intermediate phase; in particular there is no pyrochlore-type phase at this part of the RuO₂/PZT interface.

However, the PZT layer is incompletely crystallized as perovskite phase: a layer approx 50 nm thick has been stranded as a nanocrystalline pyrochlore-type structure; indicated by small bright contrast regions in the dark-field image (Figs.2,4) about 5-7.5nm diameter. The corresponding HRTEM image showed apparently randomly-oriented nanocrystals consisting of 10-20 lattice fringe spacings. There was also some amorphous material at this outer surface. There were also some fluctuations in intensity with respect to background for this part of the PZT layer; which is consistent with loss of PbO by evaporation during the 650C anneal.

HRTEM images of the RuO₂/SiO₂ interface showed that there were no problems with adhesion in this case; that interface was flat and continuous.

A 10nm diameter electron probe was used to obtain EDX spectra from a series of points tracing a line perpendicular to the series of interfaces; there was no evidence for interdiffusion of RuO₂ into silica or of RuO₂ into PZT and the Pb:Zr:Ti ratio showed no systematic changes as a function of distance throughout the PZT layer, even up to the outer surface. This result implies that the cation stoichiometry of the pyrochlore phase is essentially Pb₂ZrTiO_{7-x} (0<x<1).

B. PZT/Pt/Ti/SiO₂/Si

A typical bright-field cross-section is shown as Fig.7. In this case only the Pt and PZT layers remain. The PZT forms columnar grains extending from the Pt/PZT interface to the outer surface whereas the grains of Pt are relatively much wider. Here again the PZT/electrode interface is broadened somewhat by the slight curvature of the grain boundaries; this effect is relatively small here compared to the case of RuO₂/PZT just described. The original Pt surface was presumably relatively very flat compared to that of RuO₂. The Pt/PZT interface was sharp, with no evidence for another phase separating the Pt and PZT layers. There are subgrain boundaries, i.e. dislocation arrays within the PZT. A HRTEM image from an area close to the outer surface of the PZT layer showed a few pockets of incompletely crystallized material: however, in general this PZT layer was relatively very well crystallized perovskite

structure throughout; certainly more so than was the case for the PZT/RuO₂ film described above.

IV. DISCUSSION

A. Comparison of the present results with Vijay and Desu¹

An X-ray powder diffraction study of PZT/RuO₂/SiO₂/Si thin films showed that the perovskite structure of PZT initiated at 550C and was complete by 600C. In addition to the PZT perovskite and RuO₂ peaks, there were other peaks characteristic of a cubic pyrochlore phase ($a=1.06\text{nm}$): Vijay and Desu interpreted these as due to Pb₂Ru₂O_{7-x}; asserting that this was consistent with Rutherford backscattering (RBS) depth profile results from the same films; which showed some diminution of Ru close to the PZT/RuO₂ interface. Our results showed no pyrochlore phase at the PZT/RuO₂ interface; rather nanocrystallites of a pyrochlore phase appeared at the top surface of the PZT. This often happens with sol-gel thin films if there is insufficient excess Pb added to the sol-gel precursor solution¹⁰. It is also well-known that a nanocrystalline pyrochlore phase occurs as an intermediate step during the crystallization of the PZT thin films (see e.g. Ref.¹¹).

Note also that if the partial pressure of oxygen is too high or too low during annealing then the nonstoichiometric pyrochlore phase Pb₂ZrTiO_{7-x}, $x \neq 1$, is stabilized; rather than stoichiometric Pb₂(Zr_xTi_{1-x})O₆, as required for the perovskite structure. Experimental demonstration of this point was given in a recent paper by Bursill and Brooks¹². Perovskite is usually stoichiometric within very narrow limits for all components.

This interpretation for the nature of the pyrochlore phase found by XRD was confirmed by our HRTEM images (Fig.6) and the EDX experiments, which showed no evidence for Ru/PZT interdiffusion. No Ru was detected at all throughout the PZT film using EDX.

In order to explain the RBS results we note simply that the curvature of the grains forming the PZT/RuO₂ interface extends over approx 5-6nm normal to the original substrate. This was most clearly seen for Fig.6, where the interface appears to have curved character with amplitude about 3nm (10 times $d_{110}=0.28\text{nm}$). This may be a pseudoperiodic minimal surface required to minimize elastic energy. Note that as this curved cusp-like interface is eroded during a RBS experiment, starting from the PZT side, there will be an apparent diminution of Ru at the PZT/RuO₂ interface.

Our results do not rule out absolutely some chemical Ru/PZT intermixing at the atomic level; e.g. the presence of a thin layer of PbRuO_3 would be difficult to detect in the HRTEM image. Use of a nanoprobe (1nm diameter), rather than the 10nm probe used for EDS analysis would provide more sensitivity.

B. Comments concerning degradation mechanisms

Unfortunately, the present experiments did not test the interfacial structures of both top and bottom electrodes, as required for capacitors and ferroelectric switching. It is our experience that the top electrodes are probably most critical for degradation properties; since after annealing, e.g. at 650C for 30min in the present case, there is some tendency to lose PbO , leaving some void space. This effect is compounded by the tendency to retain some remanent pockets of pyrochlore phase, or even amorphous or poorly crystallized material, close to the top surface of the PZT. Residual pyrochlore phase appears in most PZT thin films, more or less depending on the details of the annealing treatments (atmosphere, heating rate, time at temperature, etc). Thus, the top surface of the PZT, and hence the top electrode/PZT interface is likely to be significantly less perfect than the bottom electrode/PZT interface.

There are also reports that producing the top Pt electrode by sputtering may introduce a damaged layer at the PZT/Pt interface, involving preferential desorption of oxygen¹³. This has not yet been tested for RuO_2 /PZT electrodes; but a top electrode of RuO_2 , reactively-sputtered in the presence of oxygen, is less likely to suffer this effect.

It is interesting that, for the present pair of films, the Pt/PZT was much better crystallized than was the RuO_2 /PZT; only the latter showed pyrochlore. Nevertheless, the RuO_2 /PZT gave much better fatigue characteristics. It is not clear how the present results may be interpreted with respect to degradation properties. It appears necessary to examine films before and after fatigue experiments; to search for nanostructural changes which may be expected to occur if oxygen diffusion and trapping plays a significant role in degradation. So far, there have been no definitive studies on this point, although preliminary experiments showed no evidence for nanostructural changes at Pt/PZT interfaces (Reaney et al, unpublished results, 1992).

V. CONCLUSION

It seems clear from the present experiments that useful thin film PZT can certainly be obtained using sol-gel methods combined with reactive sputtering of RuO₂ electrodes; these appear to be structurally sound in the sense that the PZT/electrode interfaces are chemically sharp, reasonably flat and continuous. Care must be taken to minimize the presence of remanent pyrochlore phase; this can be managed, as shown by the present Pt/PZT film, although there were obvious problems with the outer surface of the RuO₂ film examined in the present work.

In searching for an explanation for the improved fatigue characteristics of RuO₂ electrodes it seems that use of essentially close-packed conducting oxide electrodes, such as RuO₂ or SrRuO₃ may well significantly reduce oxygen diffusion and trapping at the PZT/electrode interfaces.

Finally, it must be admitted that the crystalline perfection of the PZT thin films is likely to become significant at some point; thus dislocations, point defects and both neutral and charged small defect clusters may all interact with polar domain walls during switching and hence contribute to fatigue and other degradation phenomena. Probably, these (bulk) effects may only become evident when electrode/PZT interfaces have first been produced in a rather more controlled and reproducible manner than is generally the case at present.

This work was supported financially by the Swiss National Funds for Research and the Australian Research Council. We are grateful for the enthusiastic support Professor Nava Setter, Laboratoire de Ceramique, EPFL and Dr Pierre Stadelmann of Institut Interdepartementale de Microscopie Electronique, EPFL.

REFERENCES

- * Permanent Address: School of Physics, The University of Melbourne, Parkville
Vic., 3052, Australia
- ¹ D.P. Vijay and S.B. Desu, Appl. Phys. Letts., in press (1993).
 - ² I.K. Yoo and S.B. Desu, Phys. Stat. Sol. (a) 133 (1992) 565.
 - ³ I.K. Yoo and S.B. Desu, Proc. Inter. Symp. Applic. Ferroelectrics
(ISAF-92), M. Liu, A. Safari, A. Kingon and G. Haertling (Eds.)
IEEE Proc. (1992) pp225.
 - ⁴ D.P. Vijay, C.K. Kwok, W. Pan, I.K. Yoo and S.B. Desu, Proc. Inter.
Symp. Applic. Ferroelect. (ISAF-92), M. Liu, A. Safari, A. Kingon and
G. Haertling (Eds.) IEEE Proc. (1992) pp408.
 - ⁵ S.B. Desu and I.K. Yoo, Proc. Inter. Symp. Applic. Ferroelectrics
(ISAF-92), M. Liu, A. Safari, A. Kingon and G. Haertling (Eds.) IEEE Proc.
(1992) pp412.
 - ⁶ L.D. Madsen and L. Weaver, J. Electronic Mater. 21 (1992) 93.
 - ⁷ I. Kondo, T. Yoneyama and O. Takeuaka, J. Vac. Sci. Technol. A10 (1992) 3436.
 - ⁸ I.M. Reaney and D.J. Barber, J. Micros. 160 (1990) 213.
 - ⁹ K. Sreenivas, I.M. Reaney, T. Maeder, N. Setter, C. Jagadish and
R.G. Elliman, J. Appl. Phys., in press (1993).
 - ¹⁰ I.M. Reaney, K.G. Brooks, R. Klissourska, C. Pawlaczyk and N. Setter,
J. Amer. Cer. Soc., in press (1993).
 - ¹¹ C.K. Kwok and S.B. Desu, Appl. Phys. Letts. 60 (1992) 1430.
 - ¹² L.A. Bursill and K.G. Brooks, Appl. Phys. Lett., submitted (1993).
 - ¹³ G.R. Fox, *Composition/Structure/Property Relations of
Lead-Lanthanum-Titanate Thin Films by Multi-Ion-Beam Reactive Sputtering*,
Doctoral Thesis, The Pennsylvania State University (1992).

FIGURE CAPTIONS

Fig.1 Comparison of chemical and dimensional specifications of the two PZT thin films studied herein.

Fig.2 Overview of PZT/RuO₂/SiO₂/Si thin film showing the interface structures and the texture of the RuO₂ and PZT layers.

Fig.3 Typical electron diffraction pattern of the PZT/RuO₂/SiO₂/Si thin film.

Fig.4 Enlargement of Fig.2 showing lattice fringes within the RuO₂ grains.
Note also the nanocrystalline pyrochlore layer.

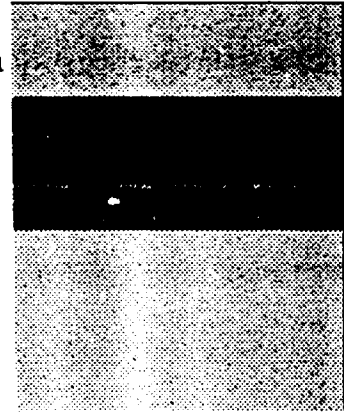
Fig.5 Detail of the RuO₂/PZT interface showing curved interphase boundaries.

Fig.6 HRTEM image of the RuO₂/PZT interface showing [101] zone axis of PZT.

Fig.7 Overview of the PZT/Pt/Ti/SiO₂/Si thin film showing the interface structures and the texture of the Pt and PZT layers.

Si/SiO₂/RuO₂/PZT

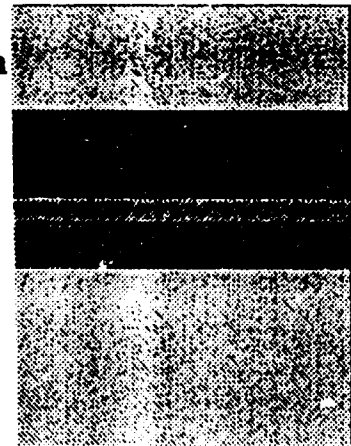
PbZr_xTi_{1-x}O₃, x=0.53 400nm thin film
RuO₂ bottom electrode 250nm
SiO₂ barrier layer 100nm
Si substrate



PZT
RuO₂
SiO₂
Si

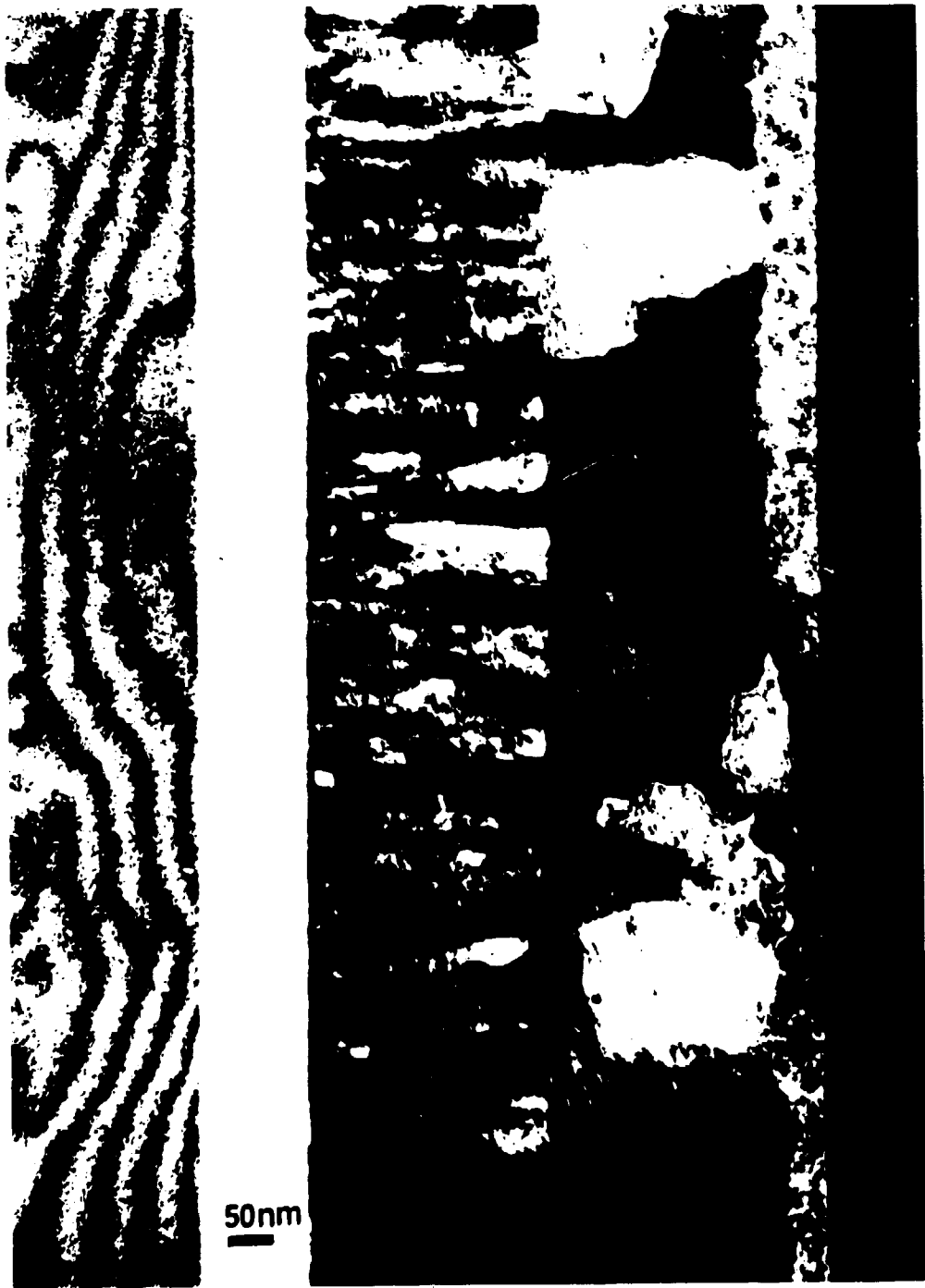
Si/SiO₂/Ti/Pt/PZT

PbZr_xTi_{1-x}O₃, x=0.53 400nm thin film
Pt bottom electrode 300nm
Ti adhesion layer 30nm
SiO₂ barrier layer 200nm
Si substrate



PZT
Pt
Ti
SiO₂
Si

FIG. 1



Si

SiO₂

RuO₂

PZT

Epoxy

FIG. 2

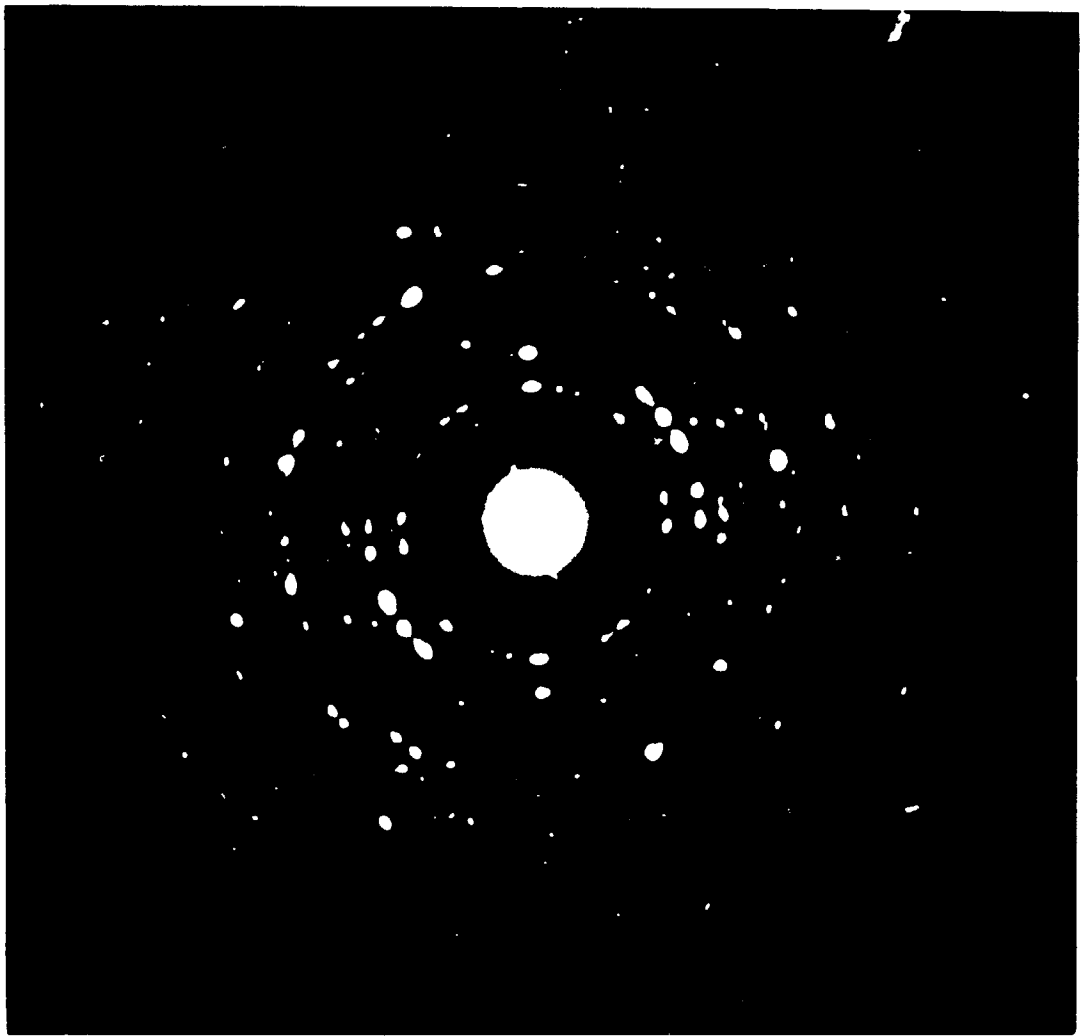


FIG. 3

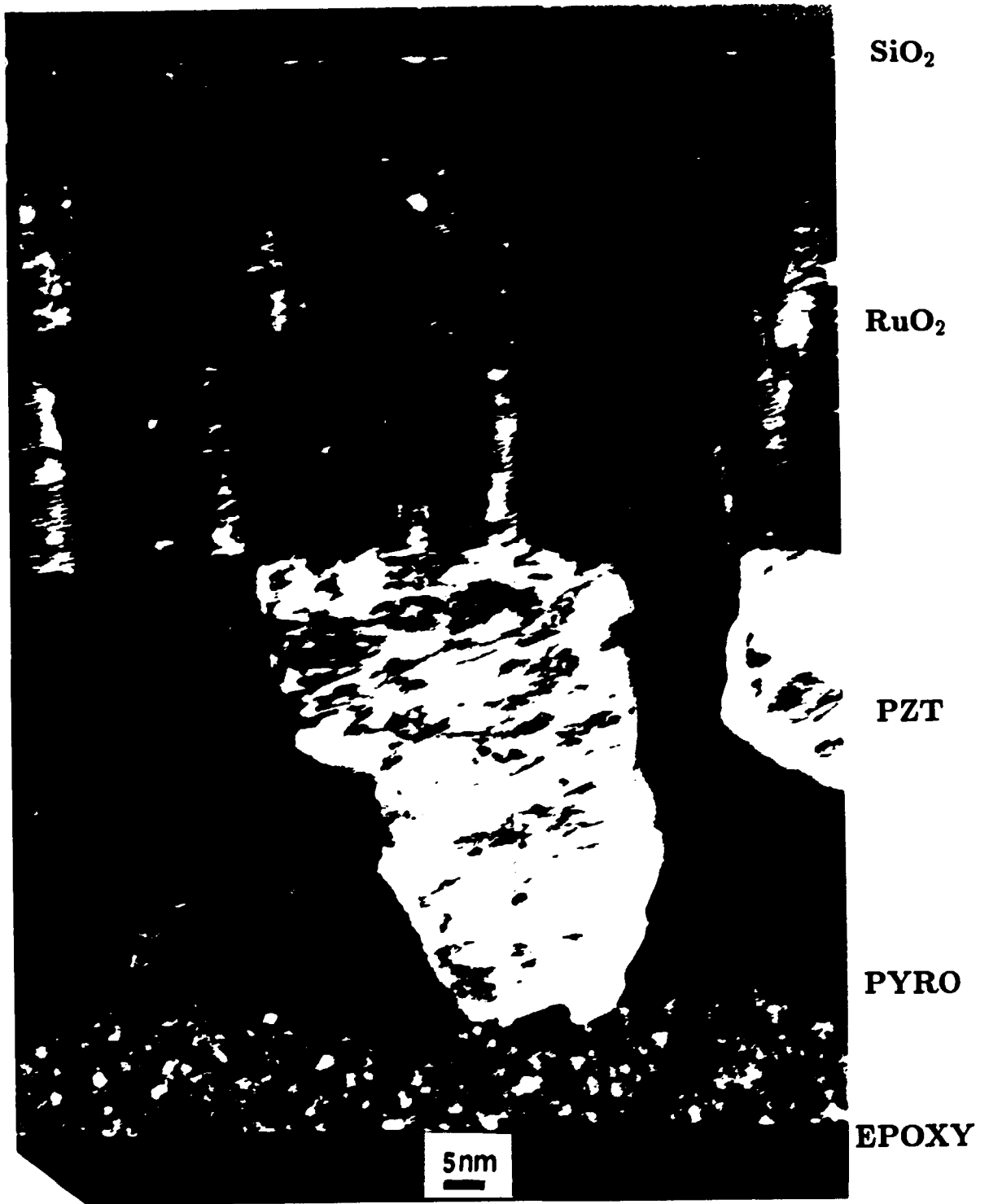


FIG. 4

Biocatalytic conversion of glucose to ethanol using a genetically modified yeast

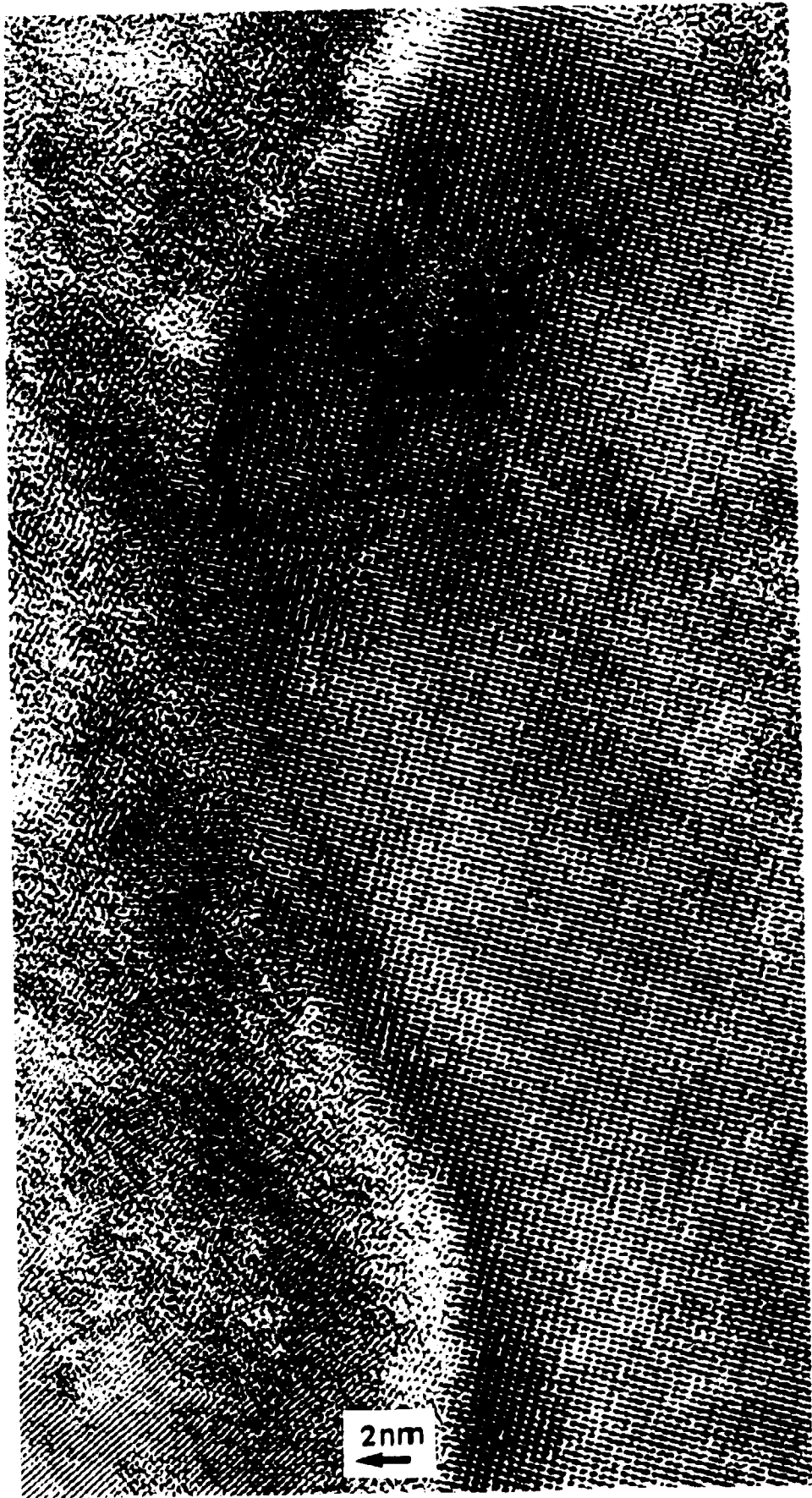


RuO₂

PZT

FIG. 5

Small-angle X-ray diffraction of PZT film



RuO₂

PZT

FIG. 6

Fig. 6



Pt

PZT

FIG. 7